Results on magnetohydrodynamics simulations with BHAC-QGP

Ashutosh Dash

Institute for Theoretical Physics, Goethe University, Frankfurt am Main

with

M. Mayer, G. Inghirami, H. Elfner, L. Rezzolla, D. H. Rischke

THIC 2025

Outline

- Broad Overview of Research Area
- Key Research Contributions and Results
- Future Research Directions and Goals
- Teaching Philosophy and Plan

Physics of Heavy-ion collision

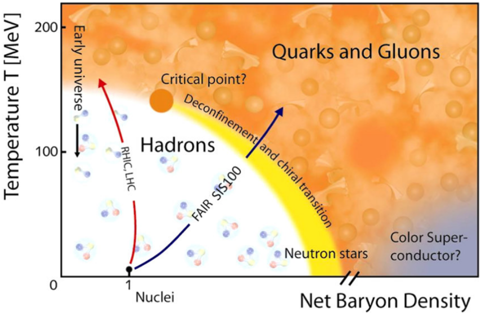

[NuPECC Long Range Plan 2017]

Emergent properties of QCD using relativistic heavy-ion collision:

- QCD transitions: De-confinement and chiral symmetry restoration.
- Deconfined state of quarks and gluons : Quark Gluon Plasma (QGP).
- Properties of QGP: viscosity, conductivity, opacity, polarization and vorticity.
- Phase diagram of QCD: Thermalization, crossover, first order, critical point ?

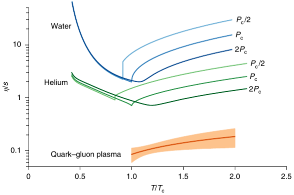

Shear Viscosity [Bernhard et al. (2019)]

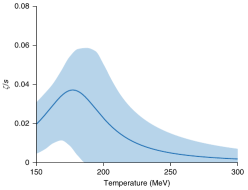

Bulk Viscosity [Bernhard et al. (2019)]

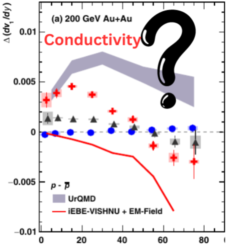

Conductivity [Abdulhamid et al. (2024)]

- Very precise estimates of QGP: shear and bulk viscosity $\pm$ errors using state-of-art Bayesian estimation has been done.
- For electrical conductivity is lacking.

Goal: Estimate the electrical conductivity of Quark-Gluon Plasma (QGP).

Different ways to calculate conductivity

CRC-TR 211

From photon/dilepton spectra

$$\lim_{p_T \to 0} \frac{dN_\gamma}{p_T \, dp_T \, d\eta} \propto \hat{\sigma}.$$

- **Perturbative method**: Kinetic theory $0.19 < \sigma/T < 2$ [Arnold et al. (2000)], [Ghiglieri et al. (2013)], [Yin (2014)]
- **Non-perturbative method**: LQCD $0.003 < \sigma/T < 0.018$ [Gupta (2004)], [Ding et al. (2011)] [Aarts and Nikolaev (2021)]

Dynamical space-time evolving QGP: `Relativistic MagnetoHyDrodynamics (RMHD)`

Relativistic MagnetoHyDrodynamics (RMHD)

Fluid conservation laws:

- Charge:

$$\partial_\alpha J^\alpha = 0$$

- Energy-momentum:

$$\partial_\alpha (T^{\alpha\beta}_{\mathsf{fl}} + T^{\alpha\beta}_{\mathsf{em}}) = 0$$

Maxwell's equation:

$$\partial_\alpha F^{\beta\alpha} = -J^\beta$$

$$\partial^*_\alpha F^{\beta\alpha} = 0$$

Relativistic MagnetoHyDrodynamics (RMHD)

Characteristic velocities:

- Fluid velocity v
- Speed of sound $\sqrt{P/\epsilon}$
- Alfvén speed $\sqrt{B^2/(\epsilon + P)}$

Plasma become relativistic when they approach the speed of light!

Ideal Vs resistive RMHD

- Force equation:

$$F^{\nu\mu}u_\mu = 0$$

- Electric and magnetic fields:

$$\boldsymbol{E} + \boldsymbol{v} \times \boldsymbol{B} = 0$$

- **Electric field:**
  - Always a function of $\boldsymbol{v}$ and $\boldsymbol{B}$.
  - Always perpendicular to $\boldsymbol{B}$.
- **Resistivity:**
  - Vanishes everywhere.

- Force equation:

$$F^{\nu\mu}u_\mu = \eta I^\nu + \eta I^\mu u_\mu u^\nu$$

- Current density:

$$\boldsymbol{J} = \gamma\eta^{-1}\left[\boldsymbol{E} + \boldsymbol{v} \times \boldsymbol{B} - (\boldsymbol{E}\cdot\boldsymbol{v})\boldsymbol{v}\right] + (\nabla\cdot\boldsymbol{E})\boldsymbol{v}$$

- **Electric field:**
  - Independent variable of the physical system.
  - Direction is not known *a priori*.
- **Resistivity:**
  - Can change spatially and over time.

Numerical issues and challenges

Compared to the classical case, this is not a simple task for a relativistic plasma, at least for the following reasons:

1. High resolution and multi-scale simulation.
2. Large inverse plasma-β parameter $(\beta^{-1} = B^2/2P)$ at the periphery of fireball.
3. The relativistic Navier-Stokes PDEs become of mixed hyperbolic/elliptic type, leading to causality violation.
4. What is the correct Ohm's law ?
5. Numerical problems in the evolution of $\boldsymbol{E}$ (stiff equations).

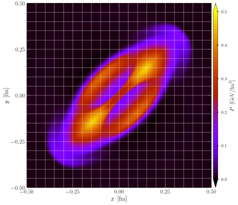

Cylindrical blast Level 1 (200×200)

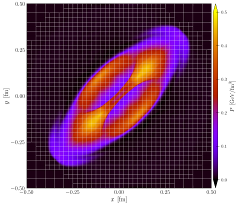

Cylindrical blast Level 2 (100×100)

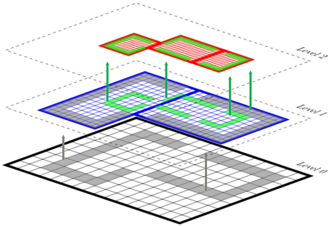

Adaptive Mesh resolution

[Mayer et al. (2024a,b)]

- Has been designed to solve the equations of ideal general-relativistic magnetohydrodynamics in arbitrary space-times
- Exploits Adaptive Mesh Refinement technique

Reduces numerical cost without sacrificing accuracy, ideal for Bayesian analysis.

Run times

Metric	W/o B (Grid: 100^3)	With B (Grid: 100^3)	With B (AMR Level = 2, Grid: 50^3)
Total Simulation Time (sec)	877.123	1034.658	782.273
Time Loop Execution Time (sec)	875.220	880.271	774.574
Regrid + Update Time (sec)	0.000	0.000	274.325
Regrid + Update (%)	0.00	0.00%	35.42%
IO Time in Loop (sec)	413.616	407.064	299.177
IO Time in Loop (%)	47.92	47.20%	38.62%
Boundary Condition (BC) Time (sec)	7.348	13.773	16.383
Boundary Condition (BC) (%)	0.83	1.60%	2.12%
Total IO Time (sec)	425.666	419.813	306.860

Table: Comparison of performance metrics for different configurations in a gird of $[-20, 20]^3$ using 64 cores.

Large inverse plasma-β parameter: Entropy switch

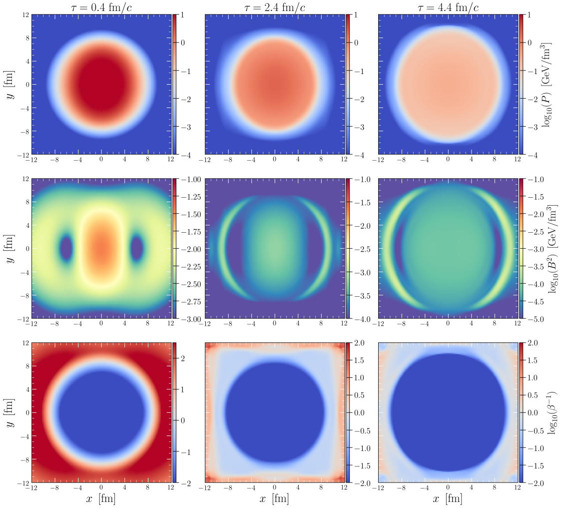

[Mayer et al. (2024a,b)]

- Numerical problem happen when magnetic pressure/kinetic pressure $>> 1$.
- BHAC-QGP can handle highly magnetized regions using entropy advection equation instead.

Code comparisions

Code	Resolution	Integrated Spectra$/(2\pi)$	Integrated v_2
`BHAC-QGP`	120^3	11.306612	2.816994
`BHAC-QGP`	200^3	11.284360	2.816532
`BHAC-QGP`	400^3	11.281298	2.818185
`ECHO-QGP`	120^3	12.048414	2.857390
`ECHO-QGP`	200^3	12.052316	2.857811
`ECHO-QGP`	400^3	12.053330	2.857962
`VHLLE`	120^3	12.744606	2.902196
`VHLLE`	200^3	12.822257	2.890757
`VHLLE`	400^3	12.871361	2.902228

Table: Comparison of integrated spectra and integrated v_2 for different codes and resolutions.

Numerical entropy production: `BHAC-QGP`$<$`ECHO-QGP`$<$`VHLLE`.

Code Comaprisions

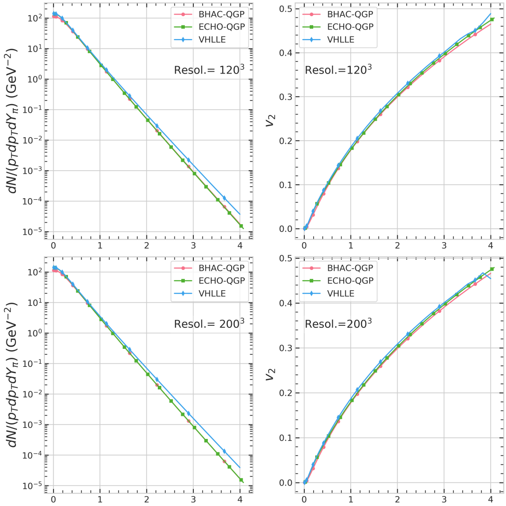

[Mayer et al. (2024a,b)]

- At low p_T `VHLLE` qualitatively agrees with `ECHO-QGP` and `BHAC-QGP`.
- For $p_T \geq 1$ `VHLLE` has a flatter spectra compared to the other two codes because of the larger production of numerical entropy.

Influence of magnetic field on particle spectra

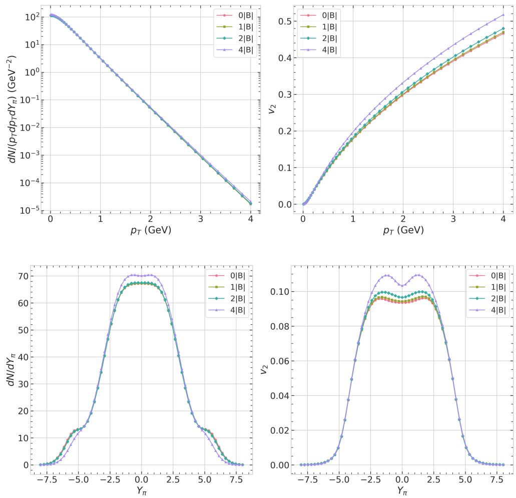

- Pure magnetic fields (ideal MHD) although strong, especially outside the fireball have no significant effect relevant for HIC.
- p_T spectra however remains unaffected.
- Stronger magnetic field leads to stronger pressure gradients and anisotropy, hence larger v_2.
- Increasing the initial magnetic field increases the pion production at mid-rapidity.
- Relativistic resistive MHD is required to do non-zero work.

Resistive MHD being a stiff problem

A **stiff problem** arises in numerical computations when there are widely varying timescales in a system of equations, such that some components evolve much faster than others.

Why Use **IMEX** (IMplicit EXplicit) Methods Over Strang Splitting?

- Treat stiff terms **implicitly** for stability.
- Treat non-stiff terms **explicitly** for efficiency.
- Avoid restrictive time step limits for stiff terms.

Resistive MHD being a stiff problem

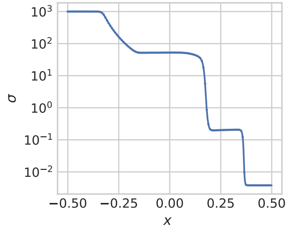

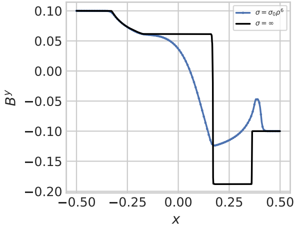

- For $x < 0$, ideal-MHD and for $x > 0$, resistive-MHD (vacuum).
- BHAC-QGP can handle non-uniform conductivity profiles even in the presence of shocks.
- Strang-splitting solutions becomes unstable beyond $\sigma > 10^4$

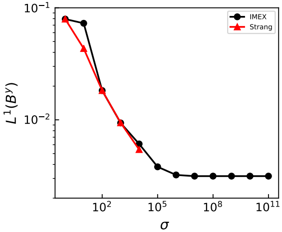

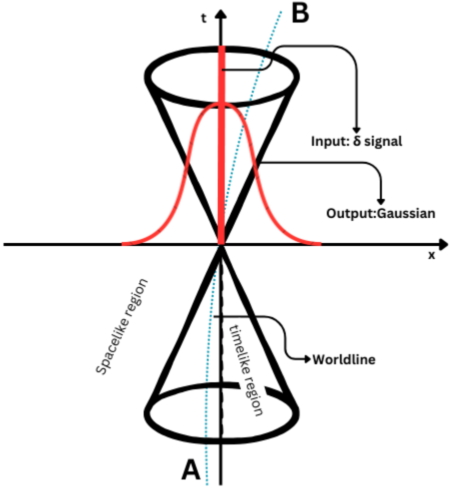

A Minkowski spacetime light cone diagram.

- Consider the classic diffusion equation, starting from equation of continuity:

$$\frac{\partial n_f(t,x)}{\partial t} + \nabla \cdot \mathbf{V}_f(t,x) = 0$$

- Use the NS form of diffusion equation $\mathbf{V}_f(t,x) = -\mathcal{D}\nabla n_f(t,x)$, yielding

$$\frac{\partial n_f(t,x)}{\partial t} = \mathcal{D}\nabla^2 n_f$$

- This is acausal !!
- Similar problem with Ohm's law: $\mathbf{V}_f(t,x) = \sigma \mathbf{E}(t,x)$

Restoring Causality

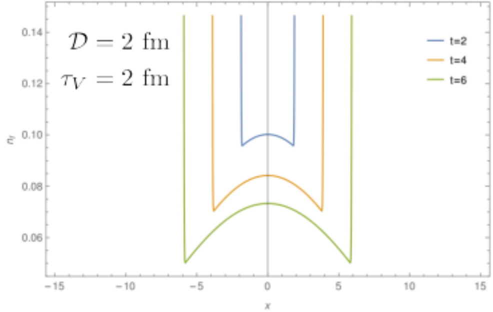

Solution to the "Telegrapher's equation"

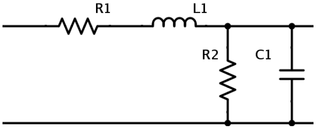

Courtesy: Oliver Heaviside

- Add a causal time lag to the diffusion equation,

$$\tau_c \frac{\partial \mathbf{V}_f(t,x)}{\partial t} + \mathbf{V}_f(t,x) = -\mathcal{D}\nabla n(t,x)$$

- τ_c is the relaxation time.

However, this can be more systematically done, using kinetic theory.

Kinetic theory and relativistic Boltzmann equation

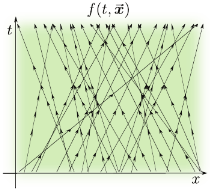

$\mathcal{C}_f = 0$ [Rezzolla, Zanotti]

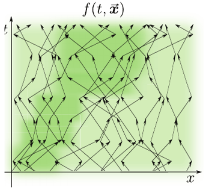

$\mathcal{C}_f \neq 0$ [Rezzolla, Zanotti]

$$p^\mu \partial_\mu f \pm q F_{\sigma\nu} p^\nu \frac{\partial}{\partial p_\sigma} f = \mathcal{C}_f$$

- Relaxation time approximation $\mathcal{C}_f := -u \cdot p (f - f_0)/\tau_c$
- Expand in gradients:

$$f = \sum_{n=0}^{\infty} \left[-\frac{\tau_c}{u \cdot p} \left(p^\mu \partial_\mu \pm q F_{\sigma\nu} p^\nu \frac{\partial}{\partial p_\sigma} \right) \right]^n f_0$$

- EoM of 2^{nd} order RMHD is obtained by suitable moments of the series, truncated at second order.

Relativistic generalization of Ohm's law

The evolution equation of diffusion current is given as:

$$\begin{aligned}\dot{V}^{\langle\mu\rangle} \;&=\; \underline{\beta_V \nabla^\mu \alpha} - \underline{\frac{V^\mu}{\tau_c}} - V_\nu \omega^{\nu\mu} - \lambda_{VV} V^\nu \sigma^\mu_\nu - \delta_{VV} V^\mu \theta + \lambda_{V\Pi} \Pi \nabla^\mu \alpha - \lambda_{V\pi} \pi^{\mu\nu} \nabla_\nu \alpha \\ &\quad - \tau_{V\pi} \pi^\mu_\nu \dot{u}^\nu + \tau_{V\Pi} \Pi \dot{u}^\mu + l_{V\pi} \Delta^{\mu\nu} \partial_\gamma \pi^\gamma_\nu - l_{V\Pi} \nabla^\mu \Pi - \underline{qB\delta_{VB} b^{\mu\gamma} V_\gamma}.\end{aligned}$$

[Mohanty et al. (2019); Dash et al. (2020); Biswas et al. (2020); Panda et al. (2021a,b)]

This is the relativistic generalisation of the Braginskii's equations, widely utilized in plasma physics and astrophysics.

[Braginskii (1965); Bessho and Bhattacharjee (2005)]

Numerical implementation

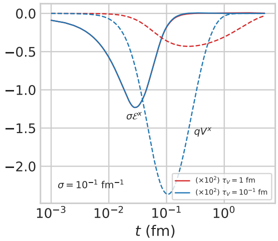

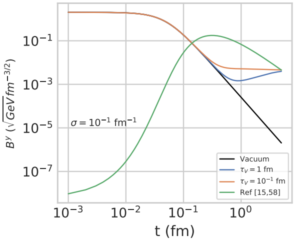

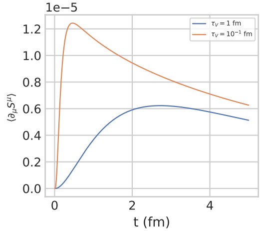

$\sigma = 10^{-1}\ \mathrm{fm}^{-1}$

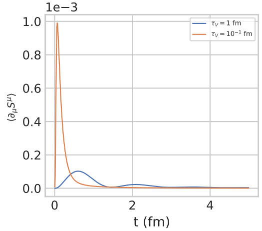

$\sigma = 10\ \mathrm{fm}^{-1}$

- Larger τ_v takes longer time to approach NS value.
- Longer τ_v means incomplete response of the charge diffusion current and hence leads to faster decay of magnetic field.
- $\partial_\mu S^\mu = -\frac{q^2}{\sigma T} V_f^\mu V_{f,\mu}$

[Dash et al. (2023)]

The effect of finite conductivity on fluid flow: Bjorken case

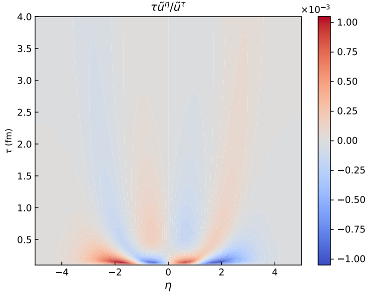

$$\sigma = 10\ \text{fm}^{-1}$$
$$\partial_\mu T^{\mu\nu}_{\mu,f} \approx 0$$

- **Initial condition**:
  1. Energy density flat with η.
  2. $u^\mu = (1,0,0,0)$.
- **Goal**: Study backreaction of EM fields.

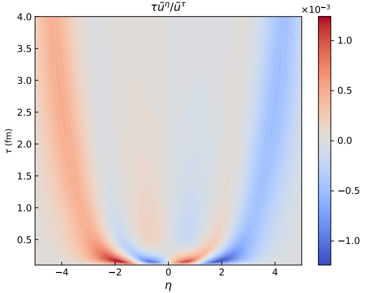

$$\sigma = 10^{-1}\ \text{fm}^{-1}$$
$$\partial_\mu T^{\mu\nu}_{\mu,f} = F^{\mu\lambda} J_{f,\lambda}$$

Summary

BHAC-QGP: Solving 3+1D Relativistic MHD Equations

- High-resolution, multi-scale simulations enabled by AMR capabilities.
- Efficient handling of large β^{-1} using an entropy switch mechanism.
- Simultaneous treatment of slow and fast variables with IMEX methods.
- The standard Navier-Stokes form of Ohm's law is acausal.

Future Work:

- Completion of a 3+1D causal second-order resistive MHD framework.
- Investigation of the dynamics of EM fields and charge diffusion with finite net charge [Parida and Chatterjee (2023)].
- Constraining the electrical conductivity σ through comparison with experimental data [Abdulhamid et al. (2024)].

Thanks for your attention

Aarts, G. and Nikolaev, A. (2021). Electrical conductivity of the quark-gluon plasma: perspective from lattice QCD. *Eur. Phys. J. A*, 57(4):118.

Abdulhamid, M. I. et al. (2024). Observation of the electromagnetic field effect via charge-dependent directed flow in heavy-ion collisions at the Relativistic Heavy Ion Collider. *Phys. Rev. X*, 14(1):011028.

Arnold, P. B., Moore, G. D., and Yaffe, L. G. (2000). Transport coefficients in high temperature gauge theories. 1. Leading log results. *JHEP*, 11:001.

Bernhard, J. E., Moreland, J. S., and Bass, S. A. (2019). Bayesian estimation of the specific shear and bulk viscosity of quark–gluon plasma. *Nature Phys.*, 15(11):1113–1117.

Bessho, N. and Bhattacharjee, A. (2005). Collisionless reconnection in an electron-positron plasma. *Phys. Rev. Lett.*, 95:245001.

Biswas, R., Dash, A., Haque, N., Pu, S., and Roy, V. (2020). Causality and stability in relativistic viscous non-resistive magneto-fluid dynamics. *JHEP*, 10:171.

Braginskii, S. I. (1965). Transport Processes in a Plasma. *Reviews of Plasma Physics*, 1:205.

Dash, A., Samanta, S., Dey, J., Gangopadhyaya, U., Ghosh, S., and Roy, V. (2020). Anisotropic transport properties of a hadron resonance gas in a magnetic field. *Phys. Rev. D*, 102(1):016016.

Dash, A., Shokri, M., Rezzolla, L., and Rischke, D. H. (2023). Charge diffusion in relativistic resistive second-order dissipative magnetohydrodynamics. *Phys. Rev. D*, 107(5):056003.

Ding, H. T., Francis, A., Kaczmarek, O., Karsch, F., Laermann, E., and Soeldner, W. (2011). Thermal dilepton rate and electrical conductivity: An analysis of vector current correlation functions in quenched lattice QCD. *Phys. Rev. D*, 83:034504.

Ghiglieri, J., Hong, J., Kurkela, A., Lu, E., Moore, G. D., and Teaney, D. (2013). Next-to-leading order thermal photon production in a weakly coupled quark-gluon plasma. *JHEP*, 05:010.

Gupta, S. (2004). The Electrical conductivity and soft photon emissivity of the QCD plasma. *Phys. Lett. B*, 597:57–62.

Mayer, M., Rezzolla, L., Elfner, H., Inghirami, G., and Rischke, D. H. (2024a). BHAC-QGP: three-dimensional MHD simulations of relativistic heavy-ion collisions, I. Methods and tests.

Mayer, M., Rezzolla, L., Elfner, H., Inghirami, G., and Rischke, D. H. (2024b). BHAC-QGP: three-dimensional MHD simulations of relativistic heavy-ion collisions, II. Application to Au-Au collisions.

Mohanty, P., Dash, A., and Roy, V. (2019). One particle distribution function and shear viscosity in magnetic field: a relaxation time approach. *Eur. Phys. J. A*, 55(3):35.

Panda, A. K., Dash, A., Biswas, R., and Roy, V. (2021a). Relativistic non-resistive viscous magnetohydrodynamics from the kinetic theory: a relaxation time approach. *JHEP*, 03:216.

Panda, A. K., Dash, A., Biswas, R., and Roy, V. (2021b). Relativistic resistive dissipative magnetohydrodynamics from the relaxation time approximation. *Phys. Rev. D*, 104(5):054004.

Parida, T. and Chatterjee, S. (2023). Baryon inhomogeneities driven charge dependent directed flow in heavy ion collisions.

Yin, Y. (2014). Electrical conductivity of the quark-gluon plasma and soft photon spectrum in heavy-ion collisions. *Phys. Rev. C*, 90(4):044903.